 DOI: 10.1002/eji.202048733 Eur. J. Immunol. 2021. 51: 354–367

Basic

European Journal of Immunology

Tissue immunology and leukocyte trafficking

Research Article

Peritoneal dialysate-range hypertonic glucose promotes T-cell IL-17 production that induces mesothelial inflammation

Alexandra Helmke[*1], *Anne M. Hüsing*[*1], *Svenja Gaedcke*[2], *Nicolas Brauns*[1], *Michael S. Balzer*[1], *Martin Reinhardt*[1], *Marcus Hiss*[1], *Nelli Shushakova*[1], *David de Luca*[2], *Immo Prinz*[3], *Hermann Haller*[1] *and Sibylle von Vietinghoff*[1]

[1] Division of Nephrology and Hypertension, Hannover Medical School, Hannover, Germany
[2] German Center for Lung Research, Hannover Medical School, Hannover, Germany
[3] Hannover Medical School, Institute for Immunology, Hannover, Germany

Peritoneal dialysis (PD) employs hypertonic glucose to remove excess water and uremic waste. Peritoneal membrane failure limits its long-term use. T-cell cytokines promote this decline. T-cell differentiation is critically determined by the microenvironment. We here study how PD-range hypertonic glucose regulates T-cell polarization and IL-17 production. In the human peritoneal cavity, $CD3^+$ cell numbers increased in PD. Single cell RNA sequencing detected expression of T helper (Th) 17 signature genes *RORC* and *IL23R*. In vitro, PD-range glucose stimulated spontaneous and amplified cytokine-induced Th17 polarization. Osmotic controls L-glucose and D-mannose demonstrate that induction of IL-17A is a substance-independent, tonicity dose-dependent process. PD-range glucose upregulated glycolysis and increased the proportion of dysfunctional mitochondria. Blockade of reactive-oxygen species (ROS) prevented IL-17A induction in response to PD-range glucose. Peritoneal mesothelium cultured with IL-17A or IL17F produced pro-inflammatory cytokines IL-6, CCL2, and CX3CL1. In PD patients, peritoneal IL-17A positively correlated with CX3CL1 concentrations. PD-range glucose-stimulated, but neither identically treated $Il17a^{-/-}Il17f^{-/-}$ nor T cells cultured with the ROS scavenger N-acetylcysteine enhanced mesothelial CX3CL1 expression. Our data delineate PD-range hypertonic glucose as a novel inducer of Th17 polarization in a mitochondrial-ROS-dependent manner. Modulation of tonicity-mediated effects of PD solutions may improve membrane survival.

Keywords: hypertonic glucose · peritoneal dialysis · peritoneal inflammation · reactive oxygen species · Th17 polarization

Additional supporting information may be found online in the Supporting Information section at the end of the article.

Correspondence: Dr. Sibylle von Vietinghoff
e-mail: vonVietinghoff.Sibylle@mh-hannover.de

*Both the authors contributed equally to this work.

Introduction

The peritoneal cavity is a model system for the study of inflammation [1]. It is lined by peritoneal mesothelial cells that readily secrete chemoattractants and protect the body from infections transmigrating from the gut or urogenital organs [2]. Clinically, its large surface, high transport capacity, and dense vascularization serve as a natural dialysis filter for patients with end stage renal disease. Approximately 15% of dialysis patients worldwide employ peritoneal dialysis (PD), which is valued for preservation of residual renal function, flexibility, and patient autonomy [3]. Excess water, electrolytes, and uremic waste are removed from the body by filling the peritoneal cavity with a sterile hypertonic solution several times per day and subsequent drainage at defined intervals. The use of PD is limited by progressive deterioration of peritoneal ultrafiltration capacity in most patients, a process that is accompanied by chronic inflammation and fibrosis [4]. Hyperosmolar glucose is the osmotic agent in the majority of PD solutions, but modern formulations contain low amounts of advanced glycation end products and the former acidic lactate buffer system is replaced by bicarbonate. However, these measures have improved peritoneal membrane survival only very moderately. Membrane failure continues to be a major unmet clinical need in PD [5].

A significant body of literature demonstrates upregulation of interleukin (IL)-17 family cytokines in PD-associated peritoneal fibrosis [1]. IL-17 contributes to host defense against infections as well as autoimmune disease and chronic inflammation. IL-17 producing T cells, which include T helper 17 (Th17) cells, γδT cells, and innate lymphoid cells [6, 7], are characterized by the transcription factor RORγt. They frequently express the closely related IL-17F, IL-21, and IL-22 cytokines in addition to IL-17A. PD patients' dialysates and peritoneal biopsies contain IL-17A. Its concentration increases in controlled conditions of murine PD models [1, 8, 9]. Antibody blockade of the IL-17A pathway significantly reduces experimental peritoneal fibrosis [8, 9]. However, the mechanisms of IL-17A induction in PD are very incompletely understood. In addition, knowledge of the mesothelial response to IL-17A is limited [1]. In many culture systems, IL-17A serves as an adjuvant to other cytokines such as TNFα rather than as a direct stimulator of endothelial or epithelial cells [1, 7]. In PD, upregulation of the Th17-related cytokines IL-6 [10] and IL-1β [11, 12] is established. Together with IL-17, they can form a self-promoting loop. Understanding the step at which PD solutions trigger this loop is essential to interrupt or prevent the proinflammatory pathophysiology of peritoneal fibrosis.

Metabolism plays a central role in regulation of T-cell IL-17 production [13]. Effector T cells, most markedly Th17 cells, upregulate glycolytic enzymes and require glycolysis for their pathophysiologic function [14–16]. Indeed, glucose concentrations that occur in diabetic patients induce Th17-type cytokine expression [17] and are part of standard T-cell culture systems (e.g., 25 mM glucose in IMDM). 25mM compared to 5.5 mM glucose significantly enhanced IL-17A production in the presence of latent TGFβ [18]. Glucose concentrations in PD fluid are markedly higher, ranging from 75.5 (1.36%) to 235.8 mM (4.25%). 1.36% and 2.27% glucose solutions are most commonly used in clinical practice [3, 5]. Glycolysis increased in mesothelial cells exposed to chronic PD solution stimulation in vivo. However, this was not replicated by PD fluid in vitro [19]. This suggests that other cell types could be responsible for mesothelial damage in vivo. As opposed to lower glucose concentrations, whether or not PD-range glucose directly activates Th17 polarization has not been reported.

Ambient tonicity is an emerging regulator of the immune response [20, 21]. Specifically, elevated NaCl concentrations favor Th17 polarization in the presence of cognate cytokines and also spontaneously [20, 22-24]. Nuclear factor of activated T cells 5 (NFAT5, also called TONEBP) was central for sensation of tonicity in this process. Most of this effect was attributed to sodium. However, minor amplifications of cytokine-mediated Th17 polarization were also observed with other hypertonic substances including Na-gluconate, $MgCl_2$, and mannitol [22]. The effect of glucose was not reported. Hypertonicity is the mechanism how PD solutions induce peritoneal ultrafiltration for excess fluid removal. The tonicity of glucose-based PD solutions closely associates with peritoneal fibrosis and ultrafiltration failure [25, 26]. In many cases, the need for highly concentrated PD solutions due to deteriorating peritoneal function appears to start a vicious circle that ultimately results in loss of membrane function and PD as renal replacement therapy. Distinguishing tonicity-mediated from metabolic effects may provide essential information in the search for optimally compatible PD solutions.

Single cell RNA sequencing of human dialysate T cells revealed an intraperitoneal Th17 population. We therefore investigated the impact of PD-range glucose on Th17 polarization and defined underlying mechanisms. Our data delineate that PD-range hypertonicity induces T-cell IL-17A production via ROS from dysfunctional mitochondria, which subsequently stimulates mesothelial cytokine production and thereby initiates a proinflammatory cascade in the peritoneal cavity.

Results

Peritoneal T-cell abundance and Th cell marker expression in human PD

T cells in the human peritoneal cavity were readily detected by flow cytometry (Fig. 1A). Their proportion among all live cells was markedly higher in stable PD patients than at PD catheter implantation (Fig. 1B), which agrees with other reports [27]. Peritoneal T-cell gating was confirmed by the absence of $CD3^+$ T cells in a long-term PD patient with Schimke's immuno-osseus dysplasia.

To assess human peritoneal T-cell polarization in PD, single cell RNA sequencing data were analyzed [19]. Gene expression patterns clearly separated T cells from other cell types (Fig. 1C and D and Supporting Information Fig. S1). Within this $CD3^+$ population, Th cell signature transcription factors were analyzed (Fig. 1E). Populations expressing Th1, Th2, and Treg signature

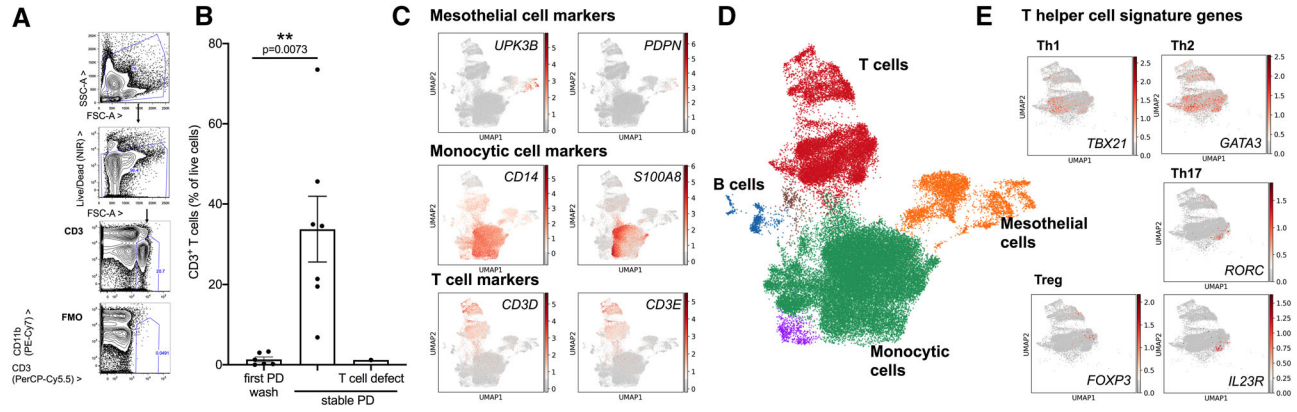

Figure 1. T-cell polarization in the human peritoneal cavity during peritoneal dialysis. (A, B) Flow cytometric analysis of CD3$^+$ T cell abundance in peritoneal dialysates from the first peritoneal lavage during catheter implantation (first PD lavage) and from stable PD patients (A, gating strategy including FMO and B, statistical analysis of $n = 6$ and 7 donors, unpaired *t*-test, cells from a T-cell deficient patient served a gating control). Data are shown as mean ± SEM. (C–E) Peritoneal single cell mRNA sequencing analysis from $n = 6$ PD patients [19]. Network-based clustering produced distinct clusters of mesothelial cells, B cells, T cells, and myeloid cells (C, selected marker genes and D, overview of classification). (E) Among CD3$^+$ cells, log-transformed expression of Th cell signature transcription factors *TBX21* (Th1), *GATA3* (Th2), *FOXP3* (Treg) and *RORC* (Th17), and the Th17 marker *IL23R* is depicted.

transcription factors as well as a population expressing the Th17 signature transcription factor RAR-related orphan receptor gamma (RORγt) and the IL-23 receptor, a marker of pathogenic Th17 cells [6, 7], were clearly detectable.

These analyses demonstrate T-cell accumulation and characteristics of Th17 cells in the peritoneal cavity of PD patients.

Spontaneous and cytokine-mediated Th17 polarization is enhanced by PD-range glucose concentrations

The impact of PD-range hypertonic glucose on T-cell polarization was tested in controlled conditions in vitro using 140 mM total glucose, closely corresponding to medium strength 2.27% PD solution (Fig. 2A). In murine splenocytes, PD-range glucose significantly increased IL-17A$^+$ among all and CD4$^+$ T cells after 4 days culture in Th17 polarizing conditions (Fig. 2B–D, gating strategy in Supporting Information Fig. S2). Polarization of isolated CD4$^+$ T cells yielded very similar results (Supporting Information Fig. S3), while it was ineffective in naïve CD4$^+$ cells ($n = 4$, data not shown). Fewer cells were recovered after culture in 140 mM glucose and indeed it significantly reduced proliferation (Supporting Information Fig. S4A–C) and also affected the proportion of dead cells detected by flow cytometry (Supporting Information Fig. S4D–G). IL-17A secretion into the supernatant increased significantly with PD-range glucose (Fig. 2E). Analyzed separately, PD-range glucose increased spontaneous IL-17A secretion already after Th0 culture without Th17-polarizing cytokines (Fig. 2E). Expression of RORγt similarly increased with PD-range glucose (Fig. 2F and G).

As an independent method, Th17 marker gene expression was investigated after culture in a range of glucose concentrations up to 140 mM glucose with and without Th0 and Th17 polarizing cytokines. Note that 140 mM glucose significantly increased spontaneous expression of Th17 signature cytokines IL-17A and IL-17F already in Th0 conditions compared to standard T-cell culture media, IMDM with 25 mM glucose (Fig. 2H). Also, RORγt mRNA expression increased glucose concentration dependently with significant effects already at 80 mM. IL-23 receptor, a marker of pathogenic Th17 cells, was similarly promoted by PD-range glucose. 140 mM glucose amplified Th17 marker expression on top of a combination of Th17-polarizing cytokines IL-6, TGF-β, and IL-1β (Fig. 2I). In contrast, expression of signature transcription factors of Th1 (T-bet, gene name *Tbx21*), Th2 (*Gata3*), and regulatory (*Foxp3*) T cells in neutral conditions was not significantly affected by PD-range glucose concentration (Supporting Information Fig. S5A–C).

These data show that PD-range glucose concentrations polarize splenocytes toward IL-17A production and further amplify the effects of Th17 differentiating cytokines.

PD-range glucose media increases glycolysis during T-cell culture

We investigated underlying mechanisms of enhanced IL-17 production in a PD-range glucose environment. Metabolic reprogramming toward glycolysis is a hallmark of Th cell differentiation [14, 28]. Indeed, culture in PD-range 140 mM compared to standard 25 mM glucose enhanced glucose consumption and lactate production (Fig. 3A and B). This was independent of Th17 polarizing cytokines.

Hypoxia-inducible factor 1 alpha (HIF-1α) is a key transcriptional regulator of glycolytic enzymes. It is known to be promoted by Th17 polarizing cytokines and mediates Th17 differentiation [28–31]. We therefore next addressed the impact of PD-range glucose on expression of HIF-1α and, as indicators of its function, central target genes that regulate the glycolysis [28] (Fig. 3C). *Hif1a* expression increased in the presence of Th17 polarizing

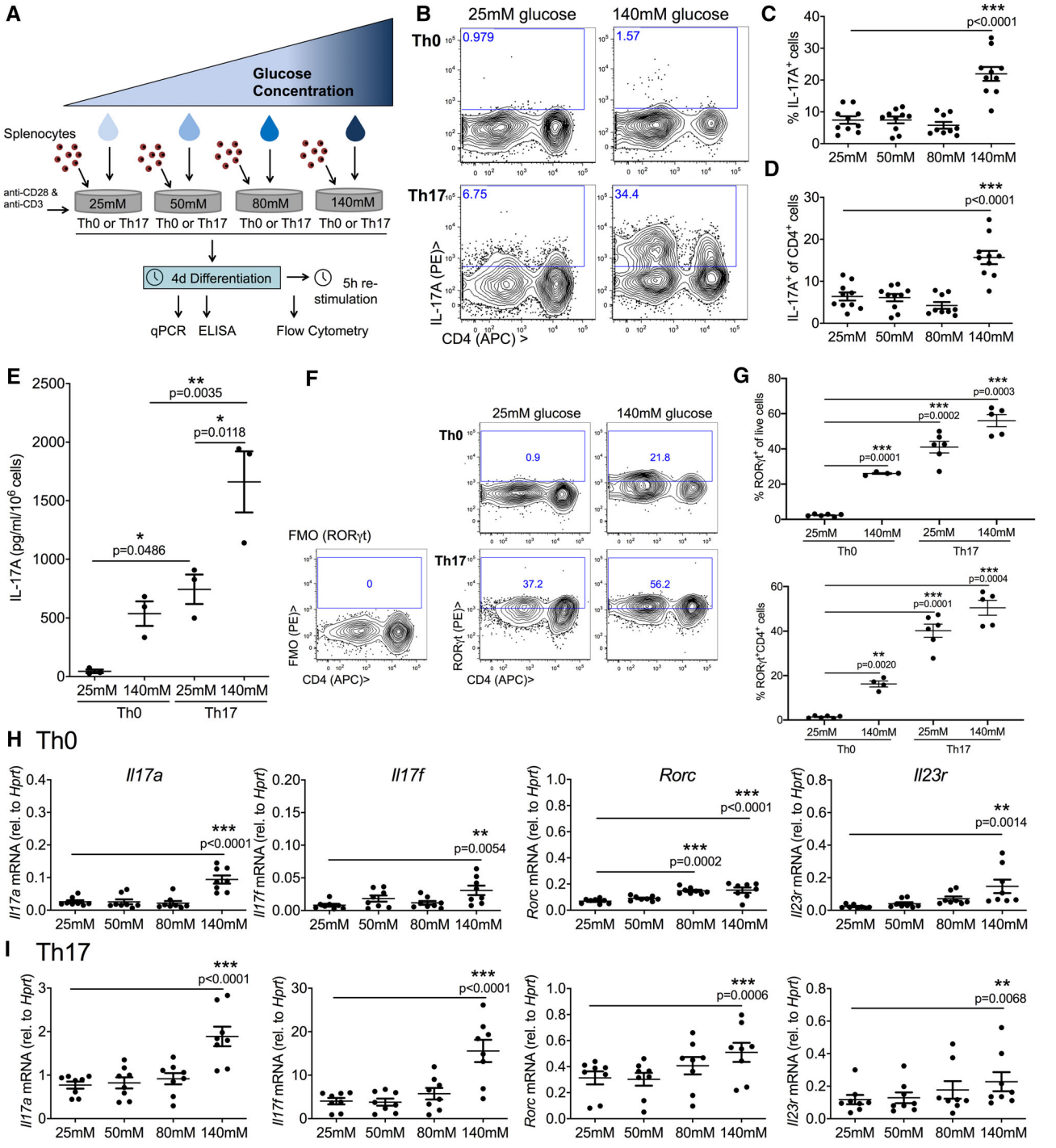

Figure 2. Role of elevated glucose concentrations for spontaneous and cytokine-mediated Th17 polarization. (A–I) WT splenocytes were cultured on anti-CD3 and anti-CD28 mAB in neutral (Th0) or Th17 polarizing conditions in standard (25 mM) or in PD-range concentrations of 50, 80, or 140 mM D-glucose (experimental design in A). (B–D) Flow cytometry was performed after restimulation and intracellular IL-17A staining (B, representative dot plots; C, D, statistical analysis of IL-17A$^+$ cells among all live cells (C) and CD4$^+$ cells (D), $n = 10$ from five independent experiments, Dunnett's after one-way ANOVA). (E) IL-17A concentration in the supernatant on day four of culture measured by ELISA (n = 3 from three independent experiments, Bonferroni after one-way ANOVA). (F, G) Assessment of RORγt protein expression by flow cytometry (F, examples; G, statistical analysis of $n = 4$–6 from two to three independent experiments, Dunnett's after ANOVA). (H, I) Expression of the Th17 marker cytokines *Il17a* and *Il17f*, Th17 signature transcription factor *Rorc*, and IL-23 receptor (*Il23r*) were assessed by qPCR relative to *Hprt* in Th0 (F) and Th17 (G) conditions ($n = 8$ from four independent experiments, Dunnett's after ANOVA). All data are shown as mean ± SEM.

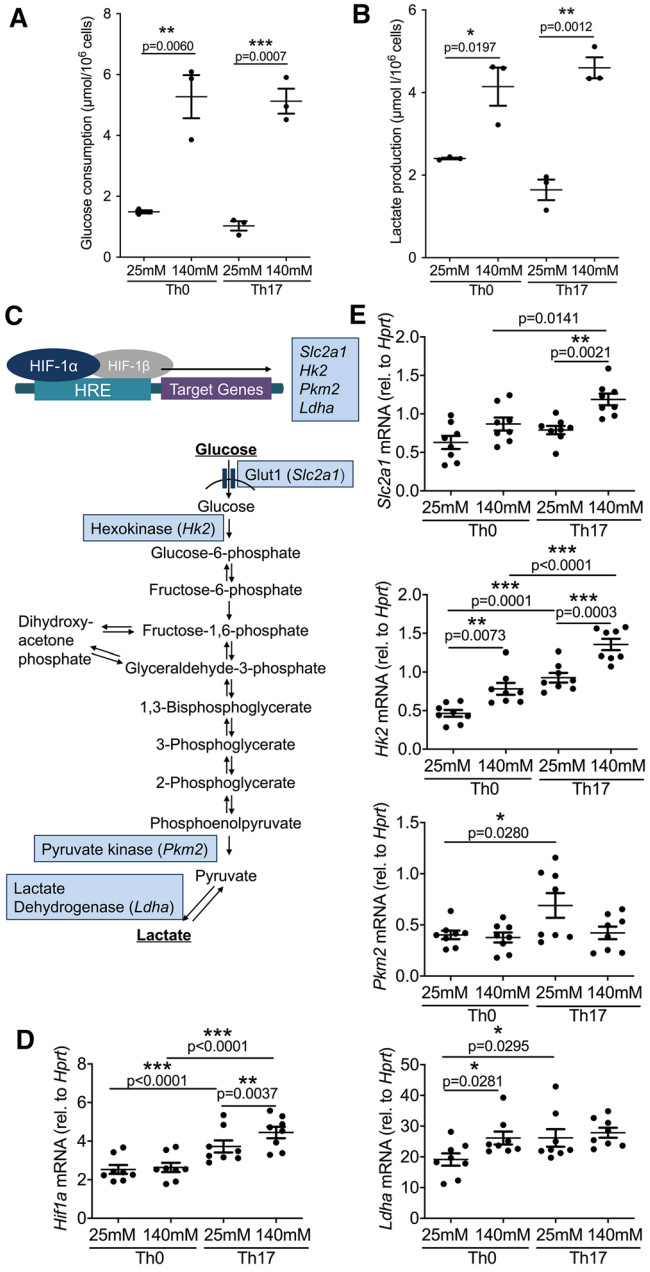

Figure 3. Glycolysis during Th17 differentiation in PD-range glucose. (A, B) Glucose consumption (A) and lactate production (B) were assessed in the cell culture medium after T-cell differentiation in standard and PD-range glucose media on anti-CD3 and anti-CD28 mAB and measured by an automated analyzer (n = 3 from three independent experiments, Bonferroni after ANOVA). (C) Overview of enzymes required in glycolysis and their regulation by HIF1α. (D, E) Gene expression analysis of *Hif1a* (D), and HIF1α-regulated glycolysis enzymes *Slc2a1*, *Hk2*, *Pkm2*, and *Ldha* (E) relative to *Hprt* after 4 days differentiation in Th0 or Th17 conditions with standard (25 mM) or PD-range (140 mM) glucose and measured by qPCR ($n = 8$ from four independent experiments, Bonferroni after one-way ANOVA). All data are shown as mean ± SEM.

cytokines. Its expression was further amplified by PD-range glucose (Fig. 3D). Similarly, expression HIF-1α target genes encoding glucose receptor 1 (*Slc2a1*), which facilitates glucose uptake, and hexokinase 2 (*Hk2*), which mediates the first step of glycolysis, was amplified by PD-range glucose (Fig. 3E). No such effect was seen for pyruvate kinase M (*Pkm2*). In addition, PD-range glucose upregulated both hexokinase 2 (*Hk2*) and lactate dehydrogenase (*Ldha*) mRNA expression already in the absence of Th17 polarizing cytokines. These data are consistent with a combination of HIF-1α-dependent and -independent effects of PD-range glucose on glycolysis regulation.

Additive effects of Th17 polarizing cytokines and PD-range glucose observed in glycolytic pathway gene expression are consistent with their cooperative effects on Th17 polarization.

Hypertonic hexose sugars elevate T-cell IL-17A production and osmotic sensor NFAT5 expression

To test whether this was caused by the abundance of D-glucose as a metabolic substrate, we employed L-glucose, the metabolically inactive stereoisomer. Using the same final total glucose concentrations, D- and L-glucose enhanced the proportion of IL-17A producing cells in indistinguishable manners (Fig. 4A and B). Also on mRNA level, IL-17A production was very similar (Fig. 4C). This argues against a direct metabolic effect of the surplus D-glucose in PD-range media as the underlying mechanism.

Standard IMDM used for T-cell polarization contains 25 mM glucose, a markedly higher concentration than in normal human plasma. We therefore conducted additional experiments in RPMI with a baseline physiological 5 mM glucose concentration (Fig. 4E). Total hexose sugar concentration was increased to PD-range (140 mM) using D-glucose, L-glucose, or D-mannose, which at a lower concentration has been reported to promote regulatory T-cell differentiation [32]. Again, the proportion of IL-17 producing T cells increased in 140 mM total hexose compared to 5 mM irrespective of the type of sugar used. These data suggest that significant effects of these hexose sugars on Th17 polarization are substance independent and may be tonicity mediated. Indeed, PD-range D-glucose increased tonicity sensor *Nfat5* mRNA expression independent of Th17 polarization in total splenocytes and isolated $CD4^+$ T cells (Fig. 4F and G). D- and L-glucose effects on *Nfat5* mRNA were very similar (Fig. 4D).

Taken together, these results propose hypertonicity as the common underlying mechanism of elevated Th17 differentiation in the presence of PD-range hexose.

PD-range glucose induces mitochondrial dysfunction

To further investigate the change in cell metabolism in a PD range glucose environment (Fig. 3A and B), we next addressed mitochondrial function. An intricate balance and interaction of mitochondrial metabolism with glycolysis modulates T-cell differentiation [28, 33].

T cells after Th0 and Th17 culture in PD-range glucose compared to control conditions were stained for dysfunctional mitochondria. Loss of mitochondrial membrane potential was significantly more frequent after exposure to PD-range glucose (Fig. 5A and B). This was equally observed for D-glucose and its

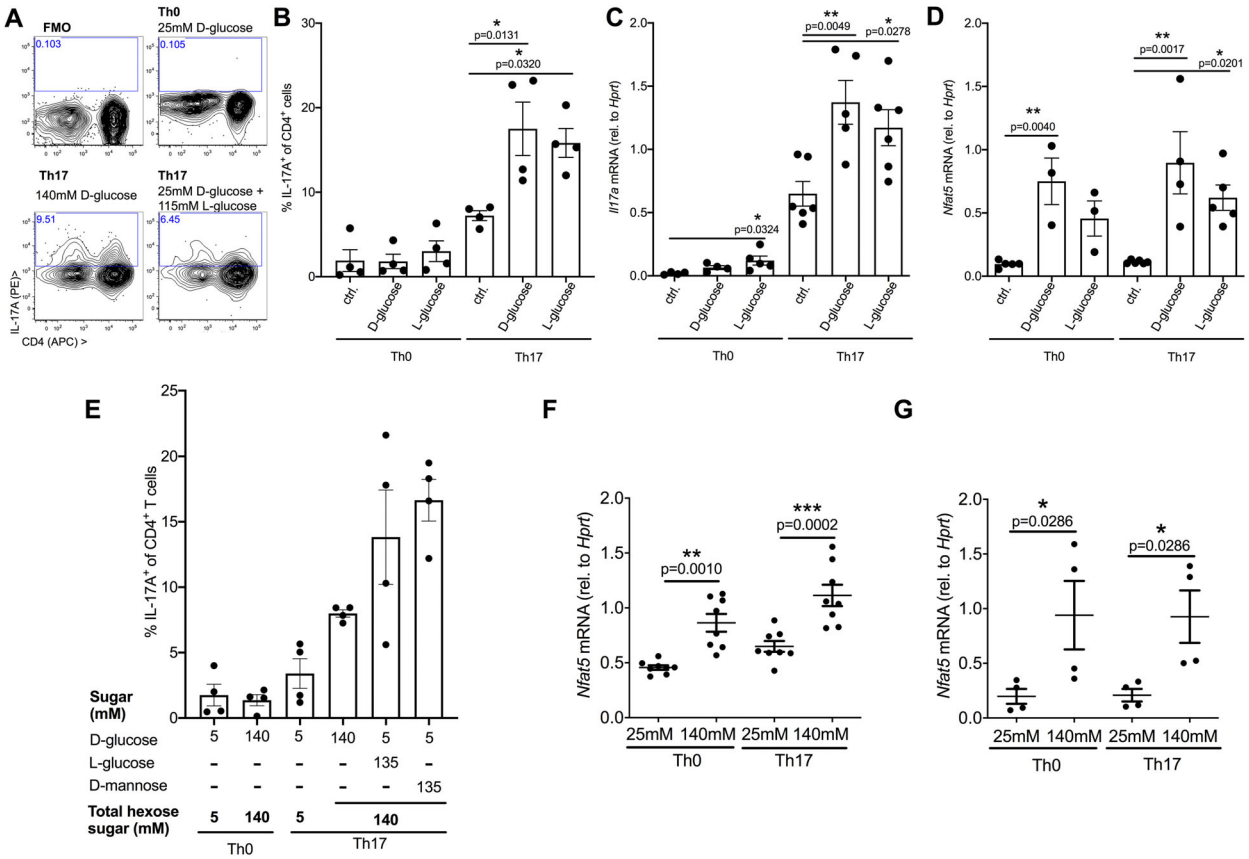

Figure 4. Role of tonicity in PD-range D-glucose, L-glucose, and D-mannose hexoses stimulated T-cell IL-17A production. (A–G) Th0 and Th17 cultures were conducted for 4 days on anti-CD3 and anti-CD28 mAB. (A–D) Total splenocytes were cultured in IMDM (25 mM D-glucose) with or without additional D- or L-glucose to reach a total of 140 mM glucose. IL-17A was assessed by flow cytometry in $CD4^+$ T cell after restimulation (A, example; B, statistical analysis) and *Il17a* (C) and *Nfat5* (D) relative to *Hprt* by qPCR ($n = 4$, two independent experiments, Dunnett's after ANOVA). (E) Total splenocyte Th0 and Th17 cultures were conducted in RPMI with a baseline of 5 mM glucose and additional D- or L-glucose or D-mannose as indicated. Flow cytometric analysis of IL-17A in $CD4^+$ T cells is shown ($n = 4$, two independent experiments). (F, G) Gene expression analysis of osmotic stress sensor NF of activated T cells 5 (*Nfat5*) in total splenocytes (F, $n = 8$, two independent experiments) and sorted $CD4^+$ T cells relative to *Hprt* by qPCR (G, $n = 4$, two independent experiments, Mann–Whitney tests). All data are shown as mean ± SEM.

metabolically inactive stereoisomer L-glucose, consistent with a tonicity-dependent process.

This shows an increase in T-cell mitochondrial dysfunction in response to PD-range hexose in vitro and in vivo.

Reactive oxygen species drive Th17 differentiation in PD-range glucose

Dysfunctional mitochondria release reactive oxygen species (ROS), which have distinct effects on immunity [28, 33, 34]. We tested whether or not ROS were involved in the observed T-cell phenotype by adding the ROS scavenger N-acetylcysteine (NAC) to Th17 differentiation in PD-range glucose. ROS scavenging dose dependently decreased the proportion of IL-17A producing among all and $CD4^+$ T cells (Fig. 5C and D). Cell viability was very good irrespective of treatment and apoptosis rates not detectably different (Supporting Information Fig. S6C and D). Posttranscriptional activation of NFAT5 protein by ROS has been reported [35]. Indeed, despite the fact that *Nfat5* mRNA expression in response to hypertonic glucose was unchanged, NAC significantly diminished IL-17A and RORγt mRNA expression (Fig. 5E and data not shown). T-cell culture in PD-range glucose without polarizing cytokines ("Th0") in the presence of NAC also resulted in much less IL-17A mRNA expression than without, despite a similar or even enhanced rise in NFAT5 mRNA (Fig. 5F and G). Human leukocytes also expressed significantly less RORγt mRNA after T-cell culture in the presence of NAC than without (Fig. 5H). In high glucose conditions, this was equally achieved by inhibition of mitochondrial ROS, which was not effective in standard glucose. Conversely, NAC either did not alter or even enhanced Th1, Th2, and regulatory T-cell signature transcription factor expression in standard or PD-range glucose (Supporting Information Fig. S5D–F) in human cells, while inhibition of mitochondrial ROS was ineffective. These data suggest that mitochondrial ROS are central mediators of increased Th17 differentiation in PD-range glucose.

To test whether this was a T-cell intrinsic effect, we exposed sorted murine $CD4^+$ T cells to PD-range glucose with or without NAC and a mitochondrial ROS inhibitor. In PD range glucose,

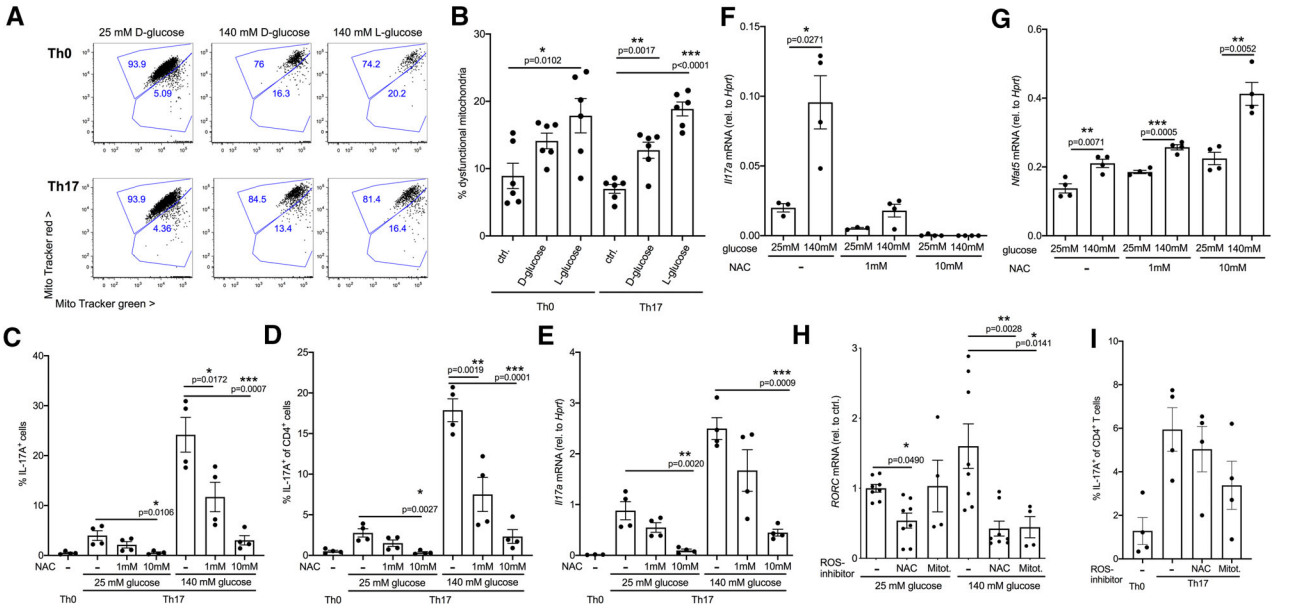

Figure 5. Mitochondrial dysfunction and the role of ROS in Th17 polarization in PD-range glucose. (A,B) After 4 days Th0 and Th17 culture on anti-CD3 and anti-CD28 mAB in the presence of the indicated concentrations of D-glucose and L-glucose, mitochondrial function was assessed by MitoTracker Green (mitochondrial lipid membranes) and MitoTracker Red (staining of respiring mitochondria) for dysfunctional mitochondria after restimulation by flow cytometry (A, typical examples and B, analysis of $n = 6$, 3 independent experiments, Dunnett's after one-way ANOVA). (C-E) After four days Th0 and Th17 cultures of total splenocytes on anti-CD3 and anti-CD28 mAB in the presence of the indicated concentrations of D-glucose and ROS scavenger N-acetylcysteine (NAC), IL-17A production was assessed by flow cytometry after restimulation and intracellular staining in all live (C) and live $CD4^+$ cells (D). IL-17A mRNA was assessed relative to *Hprt* by qPCR without restimulation. (E) ANOVA of NACs against control in each condition ($n = 4$, two independent experiments). *Il17a* (F) and *Nfat5* (G) mRNA relative to *Hprt* was assessed by qPCR after Th0 culture (*t*-tests with Welch's correction, $n = 3$-4, two independent experiments). (H) After 5 days of culture of human peripheral blood mononuclear cells on anti-CD3 and anti-CD28 mAB in the presence of the indicated concentrations of D-glucose and the presence or absence of N-acetylcysteine (NAC, 10 mM) or mitochondrial ROS inhibitor MitoTEMPO (500 μM), *RORC* mRNA was assessed relative to *Hprt* by qPCR ($n = 4$-8, two to four independent experiments, Dunnett's after ANOVA). (I) Magnetically enriched $CD4^+$ splenocytes were cultured on anti-CD3 and anti-CD28 mAB in neutral (Th0) or Th17 polarizing conditions and PD-range 140 mM D-glucose with and without ROS scavengers NAC (1 mM) or MitoTEMPO (500 μM). Flow cytometry was performed after re-stimulation and intracellular IL-17A staining on day 4 ($n = 4$, two independent experiments). All data are shown as mean ± SEM.

ROS inhibition decreased IL-17A producers with marked mitochondrial contribution, supporting the notion that indeed mitochondrial ROS are major drivers of the observed phenotype in T cells (Fig. 5I).

These data determine that T-cell mitochondrial ROS are necessary for IL-17A induction by PD-range hypertonic glucose.

IL-17A and IL-17F dose dependently stimulate peritoneal mesothelial cell cytokine production

To test for the relevance of elevated IL-17 production for peritoneal damage, we investigated mesothelial cells, which are central for PD membrane function [5]. Direct IL-17 effects on the mesothelium were studied after presence of IL-17 receptor A and the highly regulated subunit IL-17 receptor C, which are required for IL-17A and IL-17 signaling [6] was ascertained (Supporting Information Fig. S7A–C).

IL-17A in effluents of stable PD patients significantly correlated with the mesothelial chemokine CX3CL1 (fractalkine) (Fig. 6A), which we recently identified as part of a pro-fibrotic peritoneal loop [12]. To test for a functional role of IL-17A and IL-17F in mesothelial chemokine regulation, murine mesothelial cells were stimulated with recombinant cytokines. In addition to CX3CL1, we studied expression of CCL2 as mobilizer of inflammatory monocytes and Th17-related cytokines IL-1β, IL-6, TGF-β, and IL-23 (p19/p40). Importantly, direct mesothelial stimulation with PD-range glucose did not induce *Cx3cl1*, *Ccl2*, or *Il6* mRNA expression but rather downregulated expression of the former (Supporting Information Fig. S8), excluding direct effects of PD-range glucose on this mesothelial function. IL-1β and IL-23 mRNA were below detection limit in all analyzed mesothelial cell samples. Both IL-17A and IL-17F dose dependently increased mesothelial *Cx3cl1*, *Ccl2*, and *Il6* expression (Fig. 6B and C), while there was no effect on TGF-β mRNA (Supporting Information Fig. S7D and E). IL-17A maximal effect was larger, which agrees with maximal effects on other cytokines and in other cell types [6]. Both IL-17 receptor subunits A and C mRNA expression were unaffected by ligand stimulation (Supporting Information Fig. S7B and C). In line with increased gene expression levels, CX3CL1 protein in the supernatant increased (Fig. 6D). CX3CL1 also exists in a stalked form. Confocal microscopy demonstrates an increase of membrane-associated CX3CL1 on mesothelial cells after stimulation with IL-17A (Fig. 6E).

These results show that IL-17 cytokines directly promote mesothelial proinflammatory cytokine expression.

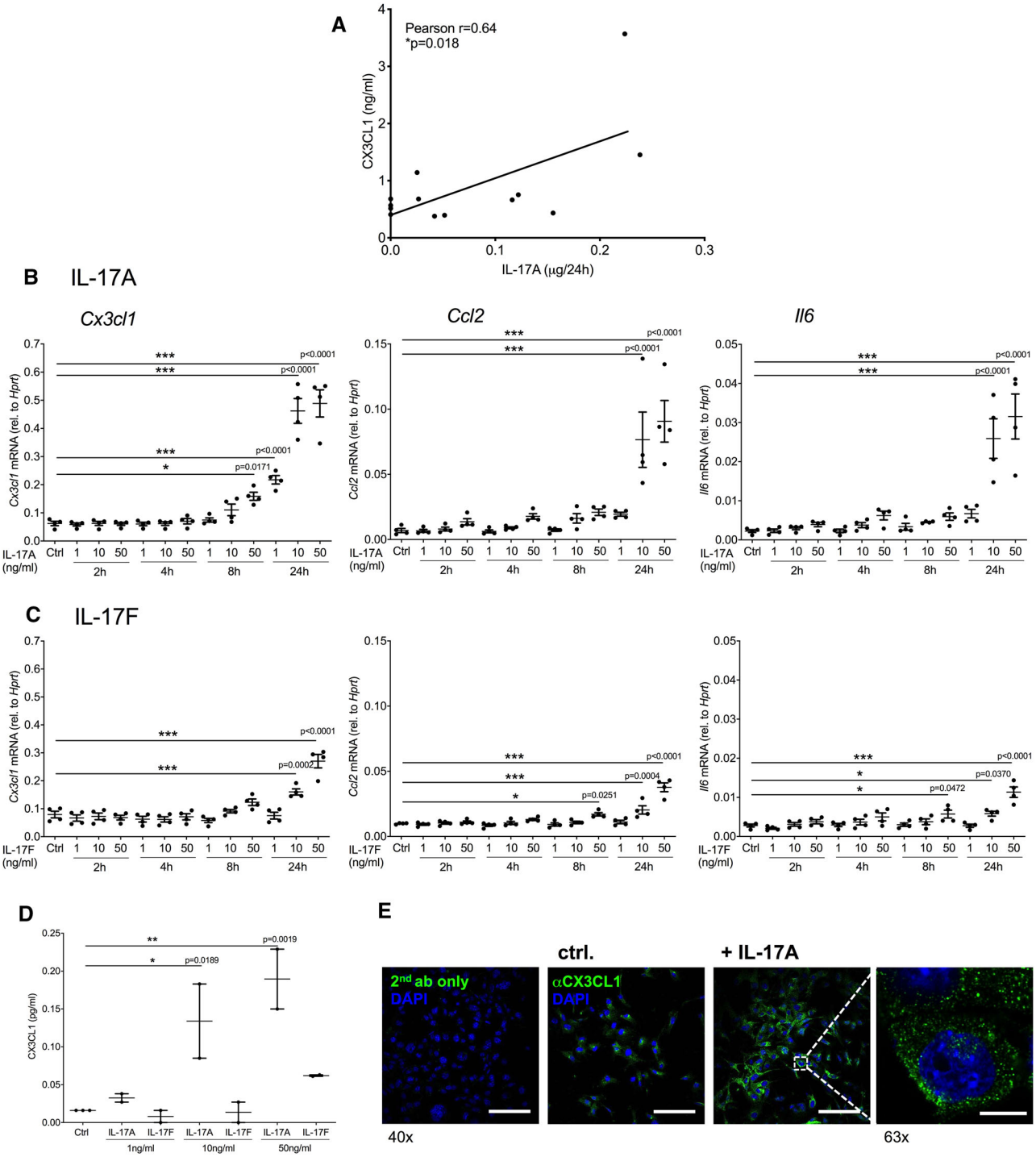

Figure 6. Effects of IL-17A and F on mesothelial cell cytokine expression. (A) The amount of IL-17A in peritoneal dialysate per day and serum CX3CL1 protein levels were measured by ELISA in peritoneal effluents of stable PD patients ($n = 13$). (B, C) Murine peritoneal mesothelial cells were stimulated with IL-17A (B) or IL-17F (C) at the indicated concentrations for 2–24 h and *Cx3cl*, *Il6*, and *Ccl2* mRNA expression relative to *Hprt* assessed by qPCR ($n = 4$, two independent experiments, Dunnett's after one-way ANOVA). (D) CX3CL1 secretion into the supernatant was assessed by ELISA after 24 h stimulation and in control cells ($n = 2$, two independent experiments, Dunnett's after ANOVA). (E) Confocal microscopy of CX3CL1 on mesothelium after 8 h stimulation with 10 ng/mL IL-17A (green = CX3CL1, blue = DAPI nuclear counterstain, one of two experiments, 40x and 63x original magnification, bars indicate 100 and 10 µm). Data are shown as mean ± SEM.

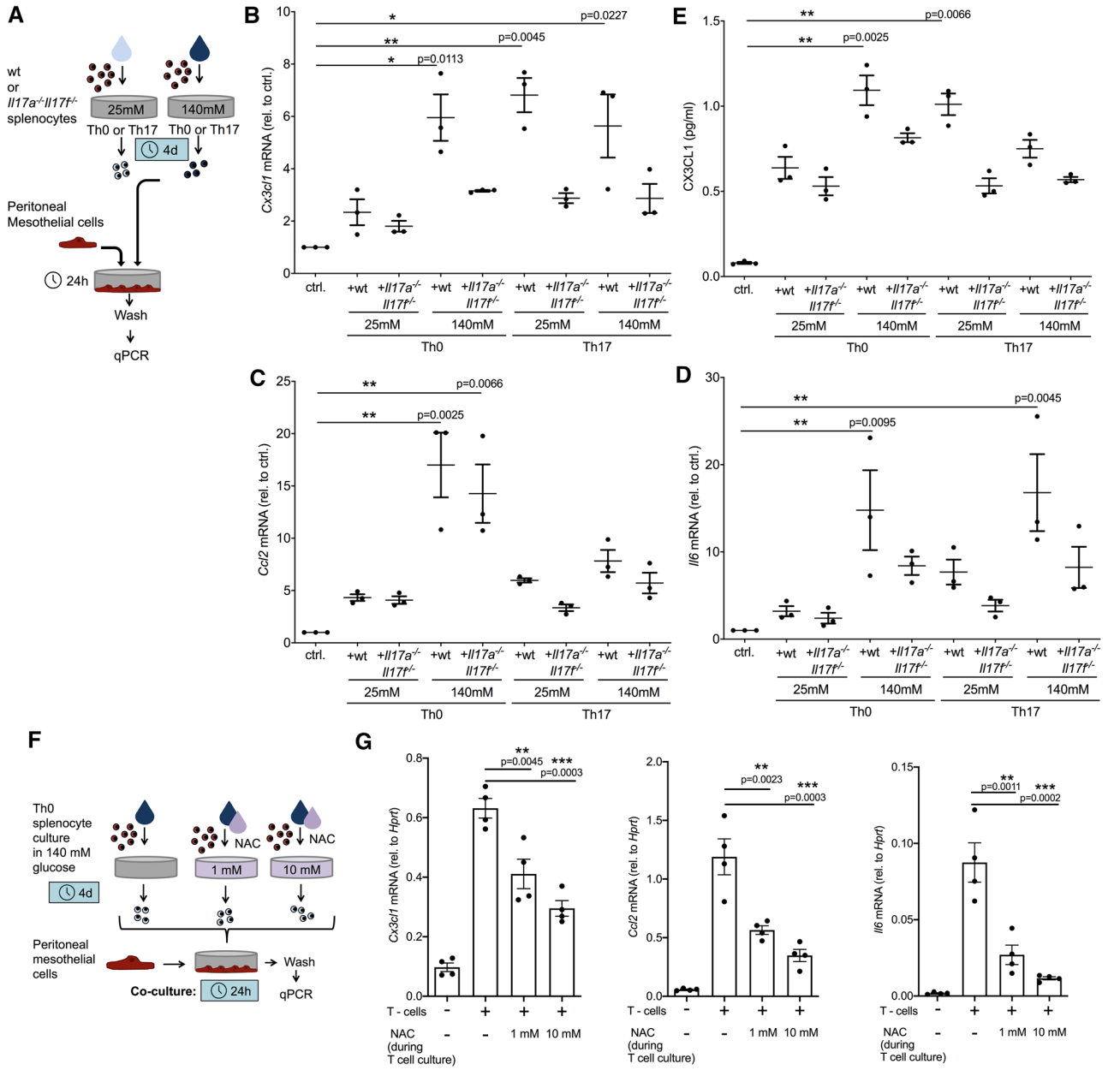

Figure 7. T cell IL-17A and IL-17F and ROS during T-cell culture in glucose-dependent induction of mesothelial CX3CL1. (A-D) WT (wt) or *Il17a*$^{-/-}$*Il17f*$^{-/-}$ splenocytes were differentiated on anti-CD3 and anti-CD28 mAB for 4 days and added to mesothelial cells 24 h before mesothelial cells were harvested and gene expression relative to *Hprt* analyzed by qPCR (experimental design depicted in A). (B–D) Gene expression analysis of mesothelial chemokines *Cx3cl1* (B), *Ccl2* (C), and *Il6* (D) ($n = 3$, two independent experiments, Dunn's after Kruskal–Wallis test). (E) CX3CL1 secretion into the supernatants of co-cultures was determined by ELISA ($n = 3$, two independent experiments, Dunn's after Kruskal–Wallis test). (F,G) WT splenocytes, which previously had been cultured on anti-CD3 and anti-CD28 mAB in 140 mM D-glucose with or without the indicated concentrations of NAC for 4 days were washed and added to peritoneal mesothelial cells for 24 h (experimental design in F). (G) Gene expression analysis by qPCR of mesothelial chemokines *Cx3cl1*, *Ccl2*, and *Il6* relative to *Hprt* ($n = 4$, 2 independent experiments, Dunnett's after one-way ANOVA). All data are shown as mean ± SEM.

IL-17A and F mediate glucose-induced T-cell effects on mesothelial CX3CL1 expression

To test whether T-cell IL-17A and IL-17F were indeed responsible for the PD-induced increase in mesothelial cytokine production, we cultured murine WT and *Il17a*$^{-/-}$*Il17f*$^{-/-}$ splenocytes with PD-range glucose during 4 days of Th0 or Th17 polarization. Mesothelial gene expression was analyzed after 24-h co-culture with these cells in standard media (Fig. 7A).

WT splenocytes cultured in PD-range glucose strongly increased mesothelial *Cx3cl1*, *Ccl2*, and *Il6* expression (Fig. 7B–D). CX3CL1 mRNA upregulation was completely abrogated if *Il17a*$^{-/-}$*Il17f*$^{-/-}$ splenocytes were used (Fig. 7B). Th17 polarizing cytokines did not alter this downstream mesothelial effect of

PD-range glucose during T-cell differentiation. Results for CX3CL1 protein secretion were very similar (Fig. 7E). These data demonstrate a mechanistic role of T-cell IL-17A and IL-17F in CX3CL1 regulation in peritoneal mesothelial cells.

Induction of mesothelial genes was replicated if washing for T cell removal was replaced by flow cytometric mesothelial cell sorting (Supporting Information Fig. S9). No effects were observed for gene expression of pro-fibrotic TGF-β1 and ECM protein collagen 1 (*Col1a1*), similar to the results after direct recombinant cytokine stimulation (Supporting Information Fig. S7D and E). T-cell IL-17A and IL-17F deficiency did not significantly alter the effect of T-cell differentiated in PD-range glucose on CCL2 or IL-6 mRNA expression (Fig. 7C and D). We therefore investigated IL-21, IL-22, and TNF-α as other Th17 signature cytokines. All three were induced by PD-range glucose to similar levels in WT and *Il17a*$^{-/-}$*Il17f*$^{-/-}$ splenocytes (Supporting Information Fig. S10). These cytokines constitute additional proinflammatory mediators excreted by T cells cultured in PD-range glucose.

In summary, these data delineate IL-17A and IL-17F as responsible cytokines for CX3CL1 induction in the mesothelium in response to T cells stimulated in hypertonic glucose.

PD-range glucose-induced T cell effects on mesothelial CX3CL1 expression require ROS

To investigate whether T-cell ROS generation was required for their detrimental action on the mesothelium, T-cells cultured for 4 days in Th0 conditions, but with PD-range glucose in the presence or absence of ROS scavenger NAC were added to mesothelial cells. Mesothelial cell chemokine expression was measured after 24-h co-culture in standard media (Fig. 7F). Indeed, induction of mesothelial *Cx3cl1*, *Ccl2*, and *Il6* was significantly lower if T cells had been incubated with an ROS scavenger during differentiation (Fig. 7G).

This demonstrates that ROS are required for differentiation of mesothelium-activating T cells in the presence of PD-range glucose.

Discussion

Our data determine glucose concentrations used for PD as novel inducers of T-cell IL-17 production and show that ROS released from damaged mitochondria are required in this process.

Our experiments show that PD-range D-glucose is sufficient to induce Th17 polarization. This was independent of additional cytokines, consistent with relevance of this finding to an environment without other inflammatory stimuli, such as the peritoneal cavity during PD. Th17 polarization was equally observed with L-glucose, the metabolically inactive stereoisomer of D-glucose and D-mannose, another hexose sugar. Expression of tonicity sensor NFAT5 was induced by all tested sugars. Thus, our results extend the range of hypertonic agents that enhance Th17 polarization [22–24] to hexoses including glucose at a concentration approved for long-term daily clinical use in humans.

In our experiments, hypertonic hexose sugars induced mitochondrial dysfunction. We show that mitochondrial ROS are instrumental for induction of IL-17 production. Inhibition of mitochondrial ROS in PD-range glucose concentrations was similarly effective in murine and human cells. As a possible mechanism, ROS were shown to directly enhance NFAT5 protein transcriptional activity [35], likely constitutes in a cooperative action together with other factors such as DNA damage [36]. Our data shed a new light on the role of ROS in T-cell differentiation; the unselective ROS scavenger NAC and even more a blocker of mitochondrial ROS effectively prevented PD-range glucose-induced Th17 generation. This agrees with recent data on Th17 regulation during an oral glucose load in vivo and in glucose levels below the PD-range in vitro [18], while results in isolated CD4$^+$ T cells in a normal glucose medium show that ROS rather impaired generation of Th17 cells [14, 37]. Our present results complement a recent publication showing that mitochondrial leakage enhanced Th17 differentiation in specific calcium channel deficient mice [38] and further support the central role of mitochondrial function in T-cell differentiation [33, 39]. Regarding its pathophysiologic role, we found that ROS scavenging during T-cell culture in PD-range glucose effectively prevented subsequent mesothelial activation. Our data thereby provide a mechanism how NAC improved experimental PD-fluid-induced peritoneal fibrosis [40].

In human peritoneal lavages, we found relatively more CD3$^+$ T cells in long-term PD patients than in incipient therapy. T cells with characteristics of effector cells and IL-17 producers were clearly detectable in agreement with others [1, 41], consistent with clinical relevance. Downstream, Th17 signature cytokines IL-17A and IL-17F both directly stimulated peritoneal mesothelial cell cytokine expression. This agrees with effects in other cell types such as renal tubular epithelium and endothelium [42]. T cells differentiated in PD-range glucose induced mesothelial CX3CL1 IL-17 dependently, delineating a direct pathophysiologic function of IL-17 in peritoneal inflammation. This is supported by the correlation of CX3CL1 with peritoneal IL-17A in vivo in humans receiving PD. An association of IL-17 with peritoneal fibrosis has been reported [8, 9], but was not reflected by direct stimulation of peritoneal mesothelial *Tgfb1* or *Col1a1* production by IL-17 in our experimental system. Our data rather suggest mesothelial pro-inflammatory cytokines as intermediate mediators of peritoneal fibrosis [12]. Along the same lines, they also propose that a recently published observation of mesothelial fibrotic mediator expression in PD in vivo but not upon direct mesothelial PD solution exposure in vitro [19] may be mechanistically related to PD-range glucose-mediated Th17 differentiation, possibly in conjunction with activation of latent TGFβ [18], as an upstream regulator of mesothelial activation in PD.

Mitochondrial function in the peritoneal cavity and in PD patients has not previously been reported. Our data demonstrate that PD-range glucose can induce mitochondrial dysfunction in T cells. Further studies should address its effect on mitochondrial function in other peritoneal cells, namely mesothelium and macrophages, but also other T-cell subtypes with currently incompletely defined roles in peritoneal fibrosis. They will also

need to determine extent and dynamics to mitochondrial reactive oxygen generation in PD conditions. Indeed, hypertonicity can disrupt mitochondrial function also in macrophages, resulting in enhanced IL-1β production [20]. Others and we demonstrated enhanced peritoneal IL-1β in murine PD models [11, 12], which, in addition to direct pathophysiologic effects, may further enhance T cell IL-17 production in PD and indeed, our data suggest that other cell types significantly promote enhanced IL-17 production in a PD-range glucose environment. Hypertonicity markedly affects mitochondrial architecture in plants [43]. Further studies, including prospectively collected peritoneal membrane samples for EM studies, are needed to evaluate this in PD patients.

Our results show that enhanced Th17 polarization by PD-range glucose is a substance independent and tonicity-dependent process, making it very unlikely that another osmotic agent will constitute a fully biocompatible PD solution [5]. On the other hand, they delineate downstream immunologic mechanisms of action of the hypertonic fluid. For some of them, such as IL-17A, specific antagonists are approved for clinical use. This does not abolish the challenges of long-term use and sheer volume of PD dialysates for any agent of peritoneal protection in PD [6]. However, oral supplementation with the ROS scavenger NAC decreased IL-17-related IL-6 levels in plasma of PD patients in a controlled study [44]. While no active clinical trials with this substance are registered at this point, our data provide a mechanism to these observations and may encourage further research of clinical outcomes, possibly with timed application after inflammatory events such as peritonitis episodes. Approaches to directly mitigate tonic stress have been tested in others areas, including the renal medulla and plant science [43, 45, 46]. In PD, they will need to take into account the undulating nature of PD-induced hypertonicity.

In conclusion, elevated tonicity as used therapeutically in PD solutions induces T-cell IL-17A production via leakage of mitochondrial ROS. IL-17 promotes CX3CL1 expression in peritoneal mesothelium contributing to a pro-inflammatory and pro-fibrotic state inside the peritoneal cavity during PD.

Materials and methods

Mice

WT C57Bl/6 and *Il17a*$^{-/-}$*Il17f*$^{-/-}$ [47] mice were genotyped by PCR and kept in specific pathogen-free conditions.

Splenocyte culture and Th17 polarization

For assessment of T-cell polarization, splenic single cell suspensions, CD4^{+}-enriched T cells (CD4^{+} T Cell Isolation Kit mouse; Miltenyi, Bergisch Gladbach, Germany) or naïve T cells (MojoSort Mouse CD4 Naive T Cell Isolation Kit; Biolegend, San Diego, CA) were used. Glucose concentrations were calculated as follows: for preparation of a stock solution in Iscove's Modified Dulbecco's media with GlutaMax (IMDM, 25 mM Glucose; Gibco, Thermo Fisher Scientific, Waltham, MA), 236 mM D-glucose or L-glucose dry substance (Sigma-Aldrich, St. Louis, MO) was added, and this media was added at a 1:1 ratio to standard full IMDM to reach a final concentration of 140 mM taking into account 1% penicillin/streptomycin and 10% FCS (PAN Biotech, Aidenbach, Germany) added after sterile filtration (FiltropurS0.2; Sarstedt, Nümbrecht, Germany). For 50 and 80 mM final glucose, 16% and 25% were added, respectively. For preparation of stock solutions in Roswell Park Memorial Institute media (RPMI, 0 mM glucose), D-glucose, L-glucose, or D-mannose dry substances were added before sterile filtration to reach a concentration of 10 mM or 270 mM hexose in the full medium containing 1% penicillin/streptomycin and 10% FCS. The cells were seeded in RPMI with 10 mmol D-glucose and the following were added at a 1:1 ratio: for 5 mM D-glucose: media without glucose. For 140 mM total hexose, either T-cell culture was on anti-CD28 (21 ng/cm^2) and anti-CD3 (212 ng/cm^2) mAB (Biolegend) for 4 days. For Th17 polarization, recombinant TGF-β1 (2 ng/mL), IL-6 (50 ng/mL; both Biolegend), IL-1β (50 ng/mL; PeproTech GmbH, Hamburg, Germany), and 5 μg/mL anti-IL-4 (11B11) and anti-IFN-γ (XMG1.2, both Biolegend) were added. D-glucose, L-glucose, D-mannose, NAC, and MitoTEMPO (((2-(2,2,6,6-Tetramethylpiperidin-1-oxyl-4-ylamino)-2-oxoethyl)triphenylphosphonium chloride) (all from Sigma-Aldrich) were added in the indicated concentrations. For determination of cell proliferation, cells were stained with carboxyfluorescein succinimidyl ester (Invitrogen, Carlsbad, CA) prior to culture.

Peritoneal mesothelial cell culture

A murine peritoneal mesothelial cell line previously generated in our laboratory was cultured as described [12] by adding 50% of a 4.25% PD solution (CAPD/DPCA3, Stay-safe; Fresenius Medical Care, Bad Homburg, Germany) to the full culture medium for 8 h or 24 h as indicated. Stimulation with recombinant murine IL-17A or IL-17F (R&D Systems, Minneapolis, MN) was for 2–24 h at the indicated concentrations.

Mesothelial cell co-culture with splenocytes

Th0- or Th17-polarized splenocytes were added to mesothelial cells (75% confluency) at 5 × 10^5 per 24 well or 2.5 × 10^6 per six well for 24 h. Cell counts were assessed using an automated analyzer (VetABC; ScilVet, Viernheim, Germany). Co-cultures were performed in full RPMI. Before mesothelial cell analysis, splenocytes were removed by washing twice with sterile PBS (Lonza, Basel, Switzerland) or by sorting mesothelial cells as live CD11b^{-}CD45^{-} cells on a FACSAriaII (Becton Dickinson, Franklin Lakes, NJ) as indicated.

Human peritoneal dialysate cytokines and leukocytes

Peritoneal IL-17A and serum CX3CL1 concentrations were measured in 13 stable PD outpatients with 6 months and less dialysis vintage [12]. Age was 53 ± 4 years, 73% female, time on renal replacement therapy 2.4 ± 0.5 months, leukocytes 6.3 ± 0.6 × 10^3/μL, CRP 9.6 ± 3.5 mg/L, weekly Kt/V 2.2 ± 0.3. Peritoneal leukocytes were assessed in peritoneal lavages obtained during PD catheter implantation ($n = 6$, 47 ± 8 years, 50% female, leukocytes 7.5 ± 2 × 10^3/μL, CRP 6.7 ± 3 mg/L) and in PD inpatients without peritonitis ($n = 7$, 54 ± 10 years, 30% female, time on renal replacement therapy 18 ± 7 months, leukocytes 7.6 ± 1.5 × 10^3/μL, CRP 28 ± 22 mg/L) immediately after drainage. Peripheral blood mononuclear cells (PBMCs) were recovered from anonymized buffy coats obtained as a waste product from the local blood donor service by density gradient centrifugation using Biocoll 1.077 (Biochrom, Berlin, Germany).

Flow cytometry

Flow cytometry was conducted in accordance with the current guidelines [48]. For flow cytometric assessment of IL-17A production, cells were restimulated with 10 ng/mL phorbol 12-myristate 13-acetate (PMA; Sigma-Aldrich) and 500 ng/mL ionomycin (Sigma-Aldrich) for 5 h. GolgiStop (BD Biosciences) was added to block cytokine export for the last 2 h of the stimulation.

The following antibodies were used: anti-mouse: anti-CD4 (GK1.5), anti-CD11b (M1/70), anti-CD45 (104), anti-TCRβ (H57-597), anti-IL-17A (TC11-18H10.1), anti-IL-17RA (PAJ-17R) (Biolegend and eBiosciences, San Diego, CA, USA), anti-RORγt (Q31-378; BD Pharmingen), anti-human: anti-CD11b (M1/70, ICRF44), anti-CD3 (UCHT1; both Biolegend). For intracellular IL-17A staining, cells were permeabilized using Fixation/Permeabilization Solution Kit (BD Biosciences), or FoxP3/Transcription Factor Staining Buffer Set (Invitrogen). Near-infrared LIVE/DEAD® Fixable Dead Cell Stain Kit (Invitrogen), MitoTracker® Green FM (for staining of total mitochondria), and MitroTracker Red CMXRos (for staining of respiring mitochondria; both from Molecular Probes®, Invitrogen detection technologies, Eugene, OR) were applied according to manufacturers' instructions. Flow cytometry analysis was performed on a Becton-Dickinson FACS Canto (BD Biosciences). Data were analyzed using FlowJo software (Tree Star Inc., Ashland, OR). The patient samples were processed at the day of the cell harvest.

RNA isolation and real-time PCR

RNA was isolated using NucleoSpin RNA Plus Kit (Macherey-Nagel, Duren, Germany) and RNA yield and purity were determined with a Colibri Microvolume Spectrometer (Titertek-Berthold, Pforzheim, Germany). After RT (M-MLV-RT; Promega, Mannheim, Germany), real-time PCR was performed on a LightCycler®96 using SYBR-Green (FastStart Taq DNA Polymerase dNTPack, Roche, Grenzach-Wyhlen, Germany). Primer sequences are listed in the supplement. *Hprt* was used as reference gene. Data were normalized to controls as indicated. Products were confirmed by melting peak analysis and gel electrophoresis. Data were analyzed using LinRegPCR software.

Immunofluorescence and confocal microscopy

For immunofluorescence staining, mesothelial cells were cultured on glass cover slips and stimulated with 10 ng/mL IL-17A (R&D Systems) for 8 h. Cells were fixed with 4% PFA and stained with polyclonal rabbit anti-mouse CX3CL1 (Abcam, Cambridge, UK) and AF555 donkey anti-rabbit IgG (Life technologies, Thermo Fisher Scientific). Confocal images were obtained with a Leica DM IRB microscope with a TCS SP2 AOBS scan head with 63× original magnification using Leica confocal software version 2.61 (Leica, Wetzlar, Germany).

Solid phase and beads ELISA

Mouse CX3CL1, human IL-17A, and human CX3CL1 Quantikine enzyme-linked immunosorbent assays (R&D Systems) were performed according to manufacturer's instructions. Cell culture supernatants were analyzed using Cytometric Bead Array mouse Th1/Th2/Th17 cytokine kit (BD biosciences) according to manufacturer's instructions. All patient samples were processed at the same time.

Assessment of glucose and lactate concentrations

Glucose and lactate concentrations in cell culture supernatants were determined using a Biosen C-line Analyzer (EKF diagnostics GmbH, Barleben, Germany) according to manufacturer's instructions. In order to determine glucose consumption, residual glucose was subtracted from initial media content. Glucose consumption and lactate production per 10^6 cells was calculated using lactate, glucose, and cell concentrations.

Analysis of human peritoneal dialysate single cell RNA sequencing data

Peritoneal dialysate single-cell data from $n = 6$ PD patients (GEO-ID: GSE130888) [19] was preprocessed with Scanpy (version 1.4.4) [49]. Cells were excluded if they expressed less than 200 genes or more than 30% of the expressed genes were mitochondrial genes. Genes were analyzed further if detected in three or more cells. The data were normalized using Scran (version 0.6.1) to produce cell-specific size factors and further log-transformed (natural log) with an offset of one. Subsequently, a batch correction was performed using ComBat (Scanpy package). The Louvain-algorithm (version 0.6.1) was employed for clustering analysis (number of neighbors for the underlying neighbor graph: 20). The marker genes per cluster were obtained by using a Wilcox's rank-sum test and compared with known marker genes

to identify underlying cell types. If multiple clusters for one cell type were found, they were merged for further analysis. From the resulting 51 887 cells, 13 198 were classified as T cells. Clusters were visualized with UMAP (version 0.3.10) and either colored by cell type or color gradient to represent the log-transformed expression of the marker genes.

Statistics

If two conditions were compared, unpaired Student's *t*-test or unpaired *t*-test with Welch's correction for samples with unequal variance was performed. If more than two conditions were compared, Dunnett's or Bonferroni's multiple comparison test after one-way ANOVA were performed as indicated. Data are displayed as mean ± SEM. *p* Values below 0.05 were considered significant and are indicated as follows: $*p < 0.05$, $**p < 0.01$, $***p < 0.001$.

Study approval

Animal use was approved by Landesamt für Verbraucherschutz und Lebensmittelsicherheit (33.19-42502-04-16/2117, Lower Saxony, Germany). Human samples were collected after written informed consent according to the declaration of Helsinki and local ethics board approval (Hannover Medical School 2010/807, 2014/6617).

Acknowledgements: We thank Martina Flechsig, Tamara Tuchel, and the Cell Sorting Core Facility at Hannover Medical School for excellent technical assistance and Dr. J. Nordlohne for help with confocal microscopy. AH, AMH, NS, DdL, IP, HH, and SvV designed research; AH, AMH, and NB conducted experiments; MSB, MR, MH, and SvV recruited patients; NS and IP provided essential reagents; AH, AMH, SG, and SvV analyzed data; and AH, AMH, SG, and SvV wrote the manuscript with help from all co-authors. Open access funding enabled and organized by Projekt DEAL.

Peer review: The peer review history for this article is available at https://publons.com/publon/10.1002/eji.202048733.

Data Availability Statement: All data sources are given in the manuscript. No high throughput/array data were generated for this work.

Conflict of interest: The authors have no commercial or financial conflict of interest.

References

1 **Witowski, J., Kamhieh-Milz, J., Kawka, E., Catar, R. and Jorres, A.**, IL-17 in peritoneal dialysis-associated inflammation and angiogenesis: conclusions and perspectives. *Front. Physiol.* 2018. **9**: 1694.

2 **Isaza-Restrepo, A., Martin-Saavedra, J. S., Velez-Leal, J. L., Vargas-Barato, F. and Riveros-Duenas, R.**, The peritoneum: beyond the tissue—a review. *Front. Physiol.* 2018. **9**: 738.

3 **Sindhu, S., Akhter, N., Arefanian, H., Al-Roub, A. A., Ali, S., Wilson, A., Al-Hubail, A. et al.**, Increased circulatory levels of fractalkine (CX3CL1) are associated with inflammatory chemokines and cytokines in individuals with type-2 diabetes. *J. Diabetes Metab Disorders* 2017. **16**: 15.

4 **Zhou, Q., Bajo, M. A., Del Peso, G., Yu, X. and Selgas, R.**, Preventing peritoneal membrane fibrosis in peritoneal dialysis patients. *Kidney Int* 2016. **90**: 515–524.

5 **Bartosova, M. and Schmitt, C. P.**, Biocompatible peritoneal dialysis: the target is still way off. *Front. Physiol.* 2018. **9**: 1853.

6 **McGeachy, M. J., Cua, D. J. and Gaffen, S. L.**, The IL-17 family of cytokines in health and disease. *Immunity* 2019. **50**: 892–906.

7 **Prinz, I., Sandrock, I. and Mrowietz, U.**, Interleukin-17 cytokines: effectors and targets in psoriasis—a breakthrough in understanding and treatment. *J. Exp. Med.* 2020. 217: e20191397.

8 **Rodrigues-Diez, R., Aroeira, L. S., Orejudo, M., Bajo, M. A., Heffernan, J. J., Rodrigues-Diez, R. R., Rayego-Mateos, S. et al.**, IL-17A is a novel player in dialysis-induced peritoneal damage. *Kidney Int.* 2014. **86**: 303–315.

9 **Ferrantelli, E., Liappas, G., Vila Cuenca, M., Keuning, E. D., Foster, T. L., Vervloet, M. G., Lopez-Cabrera, M. et al.**, The dipeptide alanyl-glutamine ameliorates peritoneal fibrosis and attenuates IL-17 dependent pathways during peritoneal dialysis. *Kidney Int* 2016. **89**: 625–635.

10 **Catar, R., Witowski, J., Zhu, N., Lucht, C., Derrac Soria, A., Uceda Fernandez, J., Chen, L. et al.**, IL-6 trans-signaling links inflammation with angiogenesis in the peritoneal membrane. *J. Am. Soc. Nephrol.* 2017. **28**: 1188–1199.

11 **Hautem, N., Morelle, J., Sow, A., Corbet, C., Feron, O., Goffin, E., Huaux, F. et al.**, The NLRP3 inflammasome has a critical role in peritoneal dialysis-related peritonitis. *J. Am. Soc. Nephrol.* 2017. **28**: 2038–2052.

12 **Helmke, A., Nordlohne, J., Balzer, M. S., Dong, L., Rong, S., Hiss, M., Shushakova, N. et al.**, CX3CL1-CX3CR1 interaction mediates macrophage-mesothelial cross talk and promotes peritoneal fibrosis. *Kidney Int.* 2019. **95**: 1405–1417.

13 **Almeida, L., Lochner, M., Berod, L. and Sparwasser, T.**, Metabolic pathways in T cell activation and lineage differentiation. *Semin. Immunol.* 2016. **28**: 514–524.

14 **Gerriets, V. A., Kishton, R. J., Nichols, A. G., Macintyre, A. N., Inoue, M., Ilkayeva, O., Winter, P. S. et al.**, Metabolic programming and PDHK1 control CD4+ T cell subsets and inflammation. *J. Clin. Invest.* 2015. **125**: 194–207.

15 **Macintyre, A. N., Gerriets, V. A., Nichols, A. G., Michalek, R. D., Rudolph, M. C., Deoliveira, D., Anderson, S. M. et al.**, The glucose transporter Glut1 is selectively essential for CD4 T cell activation and effector function. *Cell Metab.* 2014. **20**: 61–72.

16 **Sun, L., Fu, J. and Zhou, Y.**, Metabolism controls the balance of Th17/T-regulatory cells. *Front. Immunol.* 2017. **8**: 1632.

17 **Kumar, P., Natarajan, K. and Shanmugam, N.**, High glucose driven expression of pro-inflammatory cytokine and chemokine genes in lymphocytes: molecular mechanisms of IL-17 family gene expression. *Cell. Signal.* 2014. **26**: 528–539.

18 **Zhang, D., Jin, W., Wu, R., Li, J., Park, S. A., Tu, E., Zanvit, P. et al.**, High glucose intake exacerbates autoimmunity through reactive-oxygen-species-mediated TGF-beta cytokine activation. *Immunity* 2019. **51**: 671–681 e675.

19 **Si, M., Wang, Q., Li, Y., Lin, H., Luo, D., Zhao, W., Dou, X. et al.**, Inhibition of hyperglycolysis in mesothelial cells prevents peritoneal fibrosis. *Sci. Transl. Med.* 2019. 11. https://doi.org/10.1126/scitranslmed.aav5341

20 **Ip, W. K. and Medzhitov, R.**, Macrophages monitor tissue osmolarity and induce inflammatory response through NLRP3 and NLRC4 inflammasome activation. *Nat. Commun.* 2015. **6**: 6931.

21 **Muller, D. N., Wilck, N., Haase, S., Kleinewietfeld, M. and Linker, R. A.**, Sodium in the microenvironment regulates immune responses and tissue homeostasis. *Nat. Rev. Immunol.* 2019 **19**: 243–254.

22 **Kleinewietfeld, M., Manzel, A., Titze, J., Kvakan, H., Yosef, N., Linker, R. A., Muller, D. N. et al.**, Sodium chloride drives autoimmune disease by the induction of pathogenic TH17 cells. *Nature* 2013. **496**: 518–522.

23 **Wu, C., Yosef, N., Thalhamer, T., Zhu, C., Xiao, S., Kishi, Y., Regev, A. et al.**, Induction of pathogenic TH17 cells by inducible salt-sensing kinase SGK1. *Nature* 2013. **496**: 513–517.

24 **Alberdi, M., Iglesias, M., Tejedor, S., Merino, R., Lopez-Rodriguez, C. and Aramburu, J.**, Context-dependent regulation of Th17-associated genes and IFNgamma expression by the transcription factor NFAT5. *Immunol. Cell Biol.* 2017. **95**: 56–67.

25 **Kuper, C., Beck, F. X. and Neuhofer, W.**, NFAT5 contributes to osmolality-induced MCP-1 expression in mesothelial cells. *Mediators Inflamm.* 2012. **2012**: 513015.

26 **Seeger, H., Kitterer, D., Latus, J., Alscher, M. D., Braun, N. and Segerer, S.**, The potential role of NFAT5 and osmolarity in peritoneal injury. *BioMed Res. Int.* 2015. **2015**: 578453.

27 **Lewis, S. L., Bonner, P. N., Cooper, C. L. and Holmes, C. J.**, Prospective comparison of blood and peritoneal lymphocytes from continuous ambulatory peritoneal dialysis patients. *J. Clin. Lab. Immunol.* 1992. **37**: 3–19.

28 **Wang, R. and Solt, L. A.**, Metabolism of murine TH 17 cells: Impact on cell fate and function. *Eur. J. Immunol.* 2016. **46**: 807–816.

29 **Dang, E. V., Barbi, J., Yang, H. Y., Jinasena, D., Yu, H., Zheng, Y., Bordman, Z. et al.**, Control of T(H)17/T(reg) balance by hypoxia-inducible factor 1. *Cell* 2011. **146**: 772–784.

30 **Shi, L. Z., Wang, R., Huang, G., Vogel, P., Neale, G., Green, D. R. and Chi, H.**, HIF1alpha-dependent glycolytic pathway orchestrates a metabolic checkpoint for the differentiation of TH17 and Treg cells. *J. Exp. Med.* 2011. **208**: 1367–1376.

31 **Phan, A. T. and Goldrath, A. W.**, Hypoxia-inducible factors regulate T cell metabolism and function. *Mol. Immunol.* 2015. **68**: 527–535.

32 **Zhang, D., Chia, C., Jiao, X., Jin, W., Kasagi, S., Wu, R., Konkel, J. E. et al.**, D-mannose induces regulatory T cells and suppresses immunopathology. *Nat. Med.* 2017. **23**: 1036–1045.

33 **Weinberg, S. E., Sena, L. A. and Chandel, N. S.**, Mitochondria in the regulation of innate and adaptive immunity. *Immunity* 2015. **42**: 406–417.

34 **Nathan, C. and Cunningham-Bussel, A.**, Beyond oxidative stress: an immunologist's guide to reactive oxygen species. *Nat. Rev. Immunol.* 2013. **13**: 349–361.

35 **Zhou, X., Ferraris, J. D. and Burg, M. B.**, Mitochondrial reactive oxygen species contribute to high NaCl-induced activation of the transcription factor TonEBP/OREBP. *Am. J. Physiol. Renal Physiol.* 2006. **290**: F1169–F1176.

36 **Irarrazabal, C. E., Liu, J. C., Burg, M. B. and Ferraris, J. D.**, ATM, a DNA damage-inducible kinase, contributes to activation by high NaCl of the transcription factor TonEBP/OREBP. *Proc. Natl. Acad. Sci. USA* 2004. **101**: 8809–8814.

37 **Fu, G., Xu, Q., Qiu, Y., Jin, X., Xu, T., Dong, S., Wang, J. et al.**, Suppression of Th17 cell differentiation by misshapen/NIK-related kinase MINK1. *J. Exp. Med.* 2017. **214**: 1453–1469.

38 **Kaufmann, U., Kahlfuss, S., Yang, J., Ivanova, E., Koralov, S. B. and Feske, S.**, Calcium signaling controls pathogenic Th17 cell-mediated inflammation by regulating mitochondrial function. *Cell Metab.* 2019. **29**: 1104–1118 e1106.

39 **Geltink, R. I. K., Kyle, R. L. and Pearce, E. L.**, Unraveling the complex interplay between T cell metabolism and function. *Annu. Rev. Immunol.* 2018. **36**: 461–488.

40 **Noh, H., Kim, J. S., Han, K. H., Lee, G. T., Song, J. S., Chung, S. H., Jeon, J. S. et al.**, Oxidative stress during peritoneal dialysis: implications in functional and structural changes in the membrane. *Kidney Int.* 2006. **69**: 2022–2028.

41 **Roberts, G. W., Baird, D., Gallagher, K., Jones, R. E., Pepper, C. J., Williams, J. D. and Topley, N.**, Functional effector memory T cells enrich the peritoneal cavity of patients treated with peritoneal dialysis. *J. Am. Soc. Nephrol.* 2009. **20**: 1895–1900.

42 **Ahn, S. H., Edwards, A. K., Singh, S. S., Young, S. L., Lessey, B. A. and Tayade, C.**, IL-17A contributes to the pathogenesis of endometriosis by triggering proinflammatory cytokines and angiogenic growth factors. *J. Immunol.* 2015. **195**: 2591–2600.

43 **Steiner, P., Luckner, M., Kerschbaum, H., Wanner, G. and Lutz-Meindl, U.**, Ionic stress induces fusion of mitochondria to 3-D networks: an electron tomography study. *J. Struct. Biol.* 2018. **204**: 52–63.

44 **Nascimento, M. M., Suliman, M. E., Silva, M., Chinaglia, T., Marchioro, J., Hayashi, S. Y., Riella, M. C. et al.**, Effect of oral N-acetylcysteine treatment on plasma inflammatory and oxidative stress markers in peritoneal dialysis patients: a placebo-controlled study. *Peritoneal Dialys. Int.* 2010. **30**: 336–342.

45 **He, C., Yu, Z., Teixeira da Silva, J. A., Zhang, J., Liu, X., Wang, X., Zhang, X. et al.**, DoGMP1 from *Dendrobium officinale* contributes to mannose content of water-soluble polysaccharides and plays a role in salt stress response. *Sci. Rep.* 2017. **7**: 41010.

46 **Kitamura, H., Yamauchi, A., Sugiura, T., Matsuoka, Y., Horio, M., Tohyama, M., Shimada, S. et al.**, Inhibition of myo-inositol transport causes acute renal failure with selective medullary injury in the rat. *Kidney Int.* 1998. **53**: 146–153.

47 **Haas, J. D., Ravens, S., Duber, S., Sandrock, I., Oberdorfer, L., Kashani, E., Chennupati, V. et al.**, Development of interleukin-17-producing gammadelta T cells is restricted to a functional embryonic wave. *Immunity* 2012. **37**: 48–59.

48 **Cossarizza, A., Chang, H. D., Radbruch, A., Acs, A., Adam, D., Adam-Klages, S., Agace, W. W. et al.**, Guidelines for the use of flow cytometry and cell sorting in immunological studies (second edition). *Eur. J. Immunol.* 2019. **49**: 1457–1973.

49 **Wolf, F. A., Angerer, P. and Theis, F. J.**, SCANPY: large-scale single-cell gene expression data analysis. *Genome Biol.* 2018. **19**: 15.

Abbreviations: **HIF-1α**: hypoxia-inducible factor 1 alpha · **NAC**: N-acetylcysteine · **PD**: peritoneal dialysis

Full correspondence: Dr. Sibylle von Vietinghoff, Department of Nephrology and Hypertension, Hannover Medical School, OE 6840, Carl-Neuberg-Strasse 1, D-30625 Hannover, Germany
e-mail: vonVietinghoff.Sibylle@mh-hannover.de

Received: 4/5/2020
Revised: 4/8/2020
Accepted: 11/9/2020
Accepted article online: 14/9/2020